Composition of pH-Sensitive Triad in C-Lobe of Human Serum Transferrin. Comparison to Sequences of Ovotransferrin and Lactoferrin Provides Insight into Functional Differences in Iron Release†

Peter J. Halbrooks,‡ Anthony M. Giannetti,§,⊥ Joshua S. Klein,§ Pamela J. Björkman,○ Julia R. Larouche,‡ Valerie C. Smith,|| Ross T. A. MacGillivray,|| Stephen J. Everse,‡ and Anne B. Mason*,‡

Department of Biochemistry, University of Vermont, College of Medicine, Burlington, Vermont 05405, Graduate Option in Biochemistry and Molecular Biophysics, Department of Biology, and Howard Hughes Medical Institute, California Institute of Technology, Pasadena, California 91125, and Department of Biochemistry and Molecular Biology, University of British Columbia, Vancouver, British Columbia V6T 1Z3, Canada

Received September 14, 2005; Revised Manuscript Received September 29, 2005

ABSTRACT: The transferrins (TF) are a family of bilobal glycoproteins that tightly bind ferric iron. Each of the homologous N- and C-lobes contains a single iron-binding site situated in a deep cleft. Human serum transferrin (hTF) serves as the iron transport protein in the blood; circulating transferrin binds to receptors on the cell surface, and the complex is internalized by endocytosis. Within the cell, a reduction in pH leads to iron release from hTF in a receptor-dependent process resulting in a large conformational change in each lobe. In the hTF N-lobe, two critical lysines facilitate this pH-dependent conformational change allowing entry of a chelator to capture the iron. In the C-lobe, the lysine pair is replaced by a triad of residues: Lys534, Arg632, and Asp634. Previous studies show that mutation of any of these triad residues to alanine results in significant retardation of iron release at both pH 7.4 and pH 5.6. In the present work, the role of the three residues is probed further by conversion to the residues observed at the equivalent positions in ovotransferrin (Q-K-L) and human lactoferrin (K-N-N) as well as a triad with an interchanged lysine and arginine (K534R/R632K). As expected, all of the constructs bind iron and associate with the receptor with nearly the same K_D as the wild-type monoferric hTF control. However, interesting differences in the effect of the substitutions on the iron release rate in the presence and absence of the receptor at pH 5.6 are observed. Additionally, titration with KCl indicates that position 632 must have a positively charged residue to elicit a robust rate acceleration as a function of increasing salt. On the basis of these observations, a model for iron release from the hTF C-lobe is proposed. These studies provide insight into the importance of charge and geometry of the amino acids at these positions as a partial explanation for differences in behavior of individual TF family members, human serum transferrin, ovotransferrin, and lactoferrin. The studies collectively highlight important features common to both the N- and C-lobes of TF and the critical role of the receptor in iron release.

The transferrins (TF)[1] comprise a family of iron-binding proteins that include serum transferrin, ovotransferrin (oTF), and lactoferrin (LTF) (*1*). The primary function of serum transferrin synthesized by the liver and secreted into the blood plasma is iron transport. Human TF (hTF) binds Fe^{3+} and delivers it to cells via a receptor-mediated endocytotic pathway (*2*, *3*). Ovotransferrin, synthesized in the oviduct and comprising ∼12% of avian egg whites, serves as an antimicrobial agent by chelating any available Fe^{3+}, thus, depriving invading bacteria of this metal which is essential to their proliferation (*4*). Interestingly, the identical protein (differing only in the composition of the single carbohydrate)

† This work was supported by USPHS Grant R01 DK 21739 (A.B.M.) and R01-DK60770 (P.J.B.) and the Howard Hughes Medical Institute (P.J.B.). J.S.K. was supported by biology funds from the Lawrence Ferguson Endowment.

* Correspondence should be addressed to: Dr. Anne B. Mason, Department of Biochemistry, B402 Given Building, 89 Beaumont Avenue, Burlington, VT 05405. Phone, 802-656-0343; fax, 802-862-8229; e-mail, anne.mason@uvm.edu.

‡ University of Vermont.

§ Graduate Option in Biochemistry and Molecular Biophysics, California Institute of Technology.

⊥ Current address, Roche Palo Alto, LLC, Palo Alto, California 94043.

○ Department of Biology and Howard Hughes Medical Institute, California Institute of Technology.

|| University of British Columbia.

[1] Abbreviations: TF, transferrin or transferrins; hTF, human serum transferrin; oTF, ovotransferrin; LTF, lactoferrin; N-His hTF-NG, recombinant nonglycosylated human serum transferrin with a Factor Xa cleavage site and a hexa-His tag attached to the amino-terminus of the protein; N-His Y95F/Y188F hTF-NG, monoferric hTF with iron in the C-lobe; N-His Y426F/Y517F hTF-NG, monoferric hTF with iron in the N-lobe; N-His Y95F/Y188F/Y426F/Y517F hTF-NG, apo-hTF; TFR, transferrin receptor 1; sTFR, soluble transferrin receptor 1; DMEM-F12, Dulbecco's modified Eagle's medium-Ham F-12 nutrient mixture; BHK cells, baby hamster kidney cells; UG, Ultroser G; FBS, fetal bovine serum; BSA, bovine serum albumin; HRP, horseradish peroxidase; TMB, 3,3′,5,5′-tetramethylbenzidine; BA, butyric acid; Tiron, 4,5-dihydroxy-1, 3-benzenedisulfonic acid; EDTA, ethylenediamine-tetracetic acid; HEPES, *N*-(2-hydroxyethyl) piperazine-*N*′-ethanesulfonic acid; MES, morpholinoethanesulfonic acid; Ni-NTA, nickel-nitrilotriacetic acid; SPR, surface plasmon resonance; RU, resonance units; KISAB, kinetically significant anion-binding.

10.1021/bi0518693 CCC: $30.25
Published on Web 11/02/2005

also transports iron in avian plasma (*5*), thereby fulfilling two roles in a tissue specific manner. LTF, found in milk, tears, saliva, and other mammalian secretions, functions as a powerful antimicrobial agent in these secretions (*6*).

Almost all transferrins are composed of two homologous lobes designated the amino-terminal lobe (N-lobe) and the carboxyl-terminal lobe (C-lobe). The lobes share ~40% sequence identity and appear to have arisen from at least one gene duplication and fusion event (*7*). The iron-liganding residues in each lobe of oTF, LTF, and hTF are identical and are composed of an aspartic acid, two tyrosines, and a histidine. The two other ligands that make up the distorted octahedral geometry are provided by a synergistic carbonate anion, which is bound in a concomitant manner with iron (*2*). The iron is held in a cleft comprised of two subdomains (termed NI and NII, and CI and CII). Each lobe has the ability to bind Fe^{3+} reversibly in a pH-dependent manner such that iron release is accelerated at acidic pH and slowed at basic pH; factors influencing the mechanism of iron release within the cell include receptor-binding, temperature, and an as yet unidentified chelator (*8*−*10*).

Although the identical amino acids serve as ligands to the iron, there are significant differences in the iron-binding and release properties of the N- and C-lobes of any given TF and also between TF family members (*1*, *11*−*13*). For example, our recent studies document that at pH 5.6, under identical conditions, the rate of release from the C-lobe is at least 200-fold slower than the release rate from the N-lobe (*14*). The observed functional dissimilarity between lobes has been attributed to differences in the hydrogen bonding network within the cleft and the "second shell" residues (defined as amino acids that share hydrogen bonds with the iron-binding ligands) (*11*, *15*, *16*).

Analysis of the crystal structure of the hen oTF N-lobe led Dewan et al. (*12*) to propose that a pH-sensitive dilysine pair, made up of a lysine residue from domain NI and one from domain NII, might play a role in eliciting the conformational change. In the iron-containing hTF N-lobe, Lys206 is 3.04 Å from Lys296, but 9 Å apart in the apo-structure (*17*, *18*). In fact, this dilysine pair has been shown to play a key role in the mechanism leading to cleft opening and iron release (*19*, *20*). A structural feature of the two lysine residues is the presence of a "hydrophobic box" (composed of the two liganding tyrosines, Tyr95 and Tyr188, as well as Tyr85 and the histidine ligand, His249), which almost completely surrounds them. As shown in Table 1, these residues are highly conserved. This hydrophobic environment apparently changes the pK_a of one or both the lysine residues such that they are able to share a single proton at neutral pH (*19*). Mathematical and modeling studies of the N-lobe by Rinaldo and Field (*21*) emphasize the importance of the two lysines in iron release but suggest that the mechanism involves transfer of a proton from Lys296 to the nearby Tyr188 ligand which weakens the hold on iron and results in cleft opening.

The C-lobe of hTF has a triad of residues (Lys534, Arg632, and Asp634) predicted by Dewan et al. (*12*) to be important in the mechanism of iron release. Our studies have demonstrated that mutation of any of the triad residues to alanine completely inhibited iron release at pH 7.4 and slowed the rate of release substantially at pH 5.6 (*13*). Interestingly, in oTF and LTF, these three residues are not conserved (see Table 1), leading to the hypothesis that some of the altered iron release properties displayed by the C-lobes of these proteins might be due to these differences. The only studies in which iron release from these three family members has been directly compared are chemical relaxation studies by El Hage Chahine et al. (*22*−*25*). In this work, acid-induced iron release was measured and showed that hTF and oTF have proton-assisted carbonate loss from the N-lobe as the first step. Release of iron from the C-lobe seems to follow a pathway that is more complex than found for the N-lobe. Although specific differences were noted in the release rates, in the precise number of protons taken up, and in the rate-limiting steps from the C-lobes of oTF and hTF, according to these studies, they are mechanistically similar (*22*, *24*). In contrast, these chemical relaxation studies showed that the steps leading to iron release from LTF differ mechanistically from hTF and oTF (*23*).

Table 1: Alignments of Critical Residues in the N- and C-Lobes of Various TFs[a]

human TF	rabbit TF	pig TF	LTF	oTF
		N-lobe		
Glu83	Glu83	Glu82	Glu80	Glu80
Tyr85	Tyr85	Tyr84	Tyr82	Tyr82
Tyr95	**Tyr95**	**Tyr94**	**Tyr92**	**Tyr92**
Tyr188	**Tyr188**	**Tyr192**	**Tyr192**	**Tyr191**
Lys206	**Lys206**	**Lys210**	***Arg210***	**Lys209**
His249	**His249**	**His253**	**His253**	**His250**
Lys296	Lys296	Lys300	Lys301	Lys301
		C-lobe		
Glu410	Glu410	Glu414	Glu413	Glu413
Tyr412	Tyr412	Tyr416	Tyr415	Ty415
Tyr426	**Tyr425**	**Tyr431**	**Tyr435**	**Tyr431**
Tyr517	**Tyr514**	**Tyr526**	**Tyr528**	**Tyr524**
Lys534	**Lys531**	**Lys543**	**Lys546**	***Gln541***
His585	**His582**	**His594**	**His597**	**His592**
Arg632	Arg629	Arg641	*Asn644*	*Lys638*
Asp634	Asp631	Asp643	*Asn646*	*Leu640*

[a] The residues in bold designate the NII and CII subdomains in each lobe.

Binding of hTF to the specific transferrin receptor 1 (TFR) has a substantial effect on the rate of iron release, although the precise steps leading to receptor-mediated iron release from hTF are not completely clear (*26*). A number of studies have identified putative residues in both TFR and TF involved in their interaction (*27*−*29*). This work shows that specific residues within the CI domain of the C-lobe are critical to high affinity binding of hTF to the TFR. Additionally, our recent collaborative work clearly indicates that mutation of His349 in the CI domain to alanine or to a lysine residue (as found in oTF) totally eliminates the acceleration of iron release by the soluble TFR in vitro (*30*). These results demonstrate that the interaction of His349 with the TFR is essential to receptor-mediated release of the iron ~30 Å distant from this histidine and further imply an induced conformational change which leads to a stabilization of the apo-conformation.

In the current study, conversion of the K534-R632-D634 residues in hTF to the residues found at the same positions in oTF (Q-K-L) and human LTF (K-N-N) has been undertaken to help determine how the composition of the three residues influences the rate of iron release from the various C-lobes in the presence and absence of the TFR. Additionally, a K534R/R632K switch mutant was designed to alter

the geometry, without changing the charge of the two residues. In each of the full-length constructs, the two tyrosine ligands (Y95 and Y188) were mutated to phenylalanine to eliminate iron binding in the N-lobe (*31*). The ability of each recombinant monoferric hTF to bind iron, associate with the soluble TFR, and undergo pH-mediated iron release in both the presence and absence of the TFR is reported. Additionally, the effect of salt on iron release has been examined to determine whether any of the three residues might serve as an anion-binding site (*32*, *33*). Evaluation of the properties of each mutant contributes to a better understanding of the intrinsic differences between the three family members from which they are derived.

MATERIALS AND METHODS

Materials. Dulbecco's modified Eagle's medium-Ham F-12 nutrient mixture (DMEM-F12), and antibiotic-antimycotic solution (100×) were from Gibco-BRL-Life Technologies. Fetal bovine serum (FBS) was obtained from Atlanta Biologicals (Norcross, GA). Ultroser G (UG) is a serum replacement from BioSepra (Cergy, France). Bovine factor Xa was purchased from Haematologic Tecnologies, Inc. (Essex Junction, VT). The Quik-change mutagenesis kit was obtained from Strategene. Ni-NTA resin came from Qiagen. Corning expanded surface roller bottles and Dynatech Immunolon 4 Removawells were obtained from Fisher Scientific. Hi-Prep 26/60 Sephacryl S-200HR and S300HR columns were from Amersham Pharmacia. Methotrexate from Bedford Laboratories was purchased at a local hospital pharmacy and used for selection of plasmid-containing cells. Centricon 30 microconcentrators, YM-30 ultrafiltration membranes, and a spiral cartridge concentrator (CH2PRS) fitted with an S1Y10 cartridge were all from Millipore/Amicon. Bovine serum albumin (BSA) was from Sigma. Rabbit anti-mouse immunoglobulin G was from Southern Biological Associates. Immunopure NHS-LC-Biotin and immunopure avidin-horseradish peroxidase were from Pierce, as was the India His probe-HRP. The TMB Microwell peroxidase substrate system was obtained from Kirkegaard and Perry Laboratories (Gaithersburg, MD). All other chemicals and reagents were of analytical grade.

Plasmid Generation of hTF Mutants. The Quik-change protocol from Stratagene was used to introduce mutations into the hTF cDNA in the pNUT vector as described previously (*31*, *34*). All of the hTF constructs contained an N-terminal hexa-His tag and lacked N-linked glycosylation sites due to the presence of the two mutations, N413D and N611D (*31*, *34*, *35*). Additionally, each mutated triad was introduced into full-length hTF containing the Y95F/Y188F double mutant that lacks the ability to bind iron in the N-lobe (*31*). The complete DNA sequence of all clones was determined on both strands prior to transfection of the plasmid into BHK cells. As shown below, complementary mutagenic oligonucleotide primers containing the following mutations were used to introduce the desired mutations. The mutagenic nucleotides are shown in bold, underlined type:

K534Q, 5′ GAT GTG GCC TTT GTG **C**AA CAC CAG ACT GTC CC 3′; K534R, 5′ GGA GAT GTG GCC TTT GTG **AG**A CAC CAG ACT GTC 3′; R632K/D634L, 5′GAA ACC AAG GAC CTT CTG TTC A**A**A GAT **CT**C ACA GTA TGT TTG GCC 3′; and R632N/D634N, 5′GAA ACC AAG GAC CTT CTG TTC A**AT** GAT **A**A**T** ACA GTA TGT TTG GCC 3′.

Production of the single point mutants in which each member of the triad has been converted to alanine has been described in detail previously (*13*). Native ovotransferrin was purified from chicken egg white (*36*).

Production and Purification of Recombinant Proteins. Expression and purification of the recombinant hTFs was carried out as previously described (*31*). Briefly, the recombinant TFs were secreted from BHK cells into the surrounding tissue culture medium. The recombinant hTF was isolated from the media using Qiagen Ni-NTA and Sephacryl S200HR columns to yield a single band on Coomassie blue stained SDS−PAGE gels. The hTF was recovered from the S200HR column in 100 mM NH_4HCO_3, concentrated to 15 mg/mL, and stored at −20 °C until use. The amount of recombinant hTF in the tissue culture media and column eluates prior to the final step was determined by a competitive immunoassay (*37*). Following the gel filtration column, the concentration was determined by spectral analysis using extinction coefficients as previously reported (*31*). The recombinant His-tagged sTFR from the baculovirus insect cell system was expressed and purified by a similar protocol, as described in detail previously (*38*).

Removal of the Hexa-His Tag. Removal of the His tag was required for hTF samples used for the surface plasmon resonance-based binding assay in a Biacore instrument (see below) because His-tagged samples, while tightly binding to sTFR, exhibited nonconcentration-dependent response levels that could not be directly interpreted. His tag removal followed the protocol described in detail previously (*14*).

Spectral Data. To assess iron binding for each hTF, UV−vis spectra were recorded on a Varian Cary 100 spectrophotometer (600−250 nm). Difference spectra were generated by subtracting the spectrum of HEPES buffer (50 mM, pH 7.4) from the sample spectra. The reported results are the average values derived from at least three such scans.

Affinity Measurements Using Surface Plasmon Resonance. A BIACORE 2000 biosensor system (Amersham Biosciences) was used to assay the interaction between sTFR and TF as described previously (*29*, *39*). Binding of injected hTF to sTFR immobilized on the sensor chip results in changes in surface plasmon resonance that are read out in real time as resonance units (RU) (*40*, *41*). Purified sTFR was coupled to the flow cells of a CM5 sensor chip (Amersham Biosciences) using random amine coupling as previously described (*38*). Wild-type or mutant hTF was injected over the flow-cells at 70 μL/min at 25 °C in 50 mM PIPES buffer, pH 7.5, 150 mM NaCl, and 0.005% P20 surfactant. Raw sensorgram data was preprocessed using the Scrubber software package (Biologic Software Pty.; http://www.biologic.com.au) and globally fit to 2:1 or 1:1 models in Clamp 99. Results from 2:1 models were statistically corrected for better comparison with the results of the 1:1 model as previously described (*30*, *42*).

Production of hTF/sTFR Complex. A molar excess of the control N-His Y95F/Y188F hTF NG (or hTF mutants) in 100 mM NH_4HCO_3 was incubated with sTFR for 30 min at room temperature. Following passage through a 13 mm Millex-GV syringe filter (0.2 μm), each sample was loaded onto a HiPrep 26/60 Sephacryl S300HR gel filtration column (Amersham Biosciences) to separate the hTF/sTFR complex

from the free hTF. The column was equilibrated and run in 100 mM NH_4HCO_3 at a flow rate of 1−1.5 mL/min using a BioCad Sprint chromatography system, and baseline separation was achieved between the complex and the hTF. The identity of the hTF/TFR complex and the free hTF was verified by SDS−PAGE analysis on 10% gels.

Kinetics of Iron Release. As described previously in detail (*10*), the kinetics of iron removal from hTF at pH 5.6 were measured in 100 mM MES buffer using 4 mM EDTA as the chelating agent. The buffer−chelator mixture was allowed to equilibrate prior to addition of the hTF samples, and release of iron was monitored directly by following the decrease in absorbance at 293 nm on a dual-beam Cary 100 spectrophotometer equipped with a thermostable Peltier block accessory. The hTF was present at a final concentration of ∼6 μM, and all experiments were conducted at 25 °C. To ensure complete iron removal, data was collected until at least three half-lives had elapsed.

In assays involving TF/sTFR complexes, lower concentrations (∼500 nM) of protein ensured receptor solubility at the acidic pH of 5.6. A QuantaMaster Spectrofluorometer (Photon Technology International, South Brunswick NJ) was used to measure fluorescence output. This instrument is equipped with a 75-W Xenon arc lamp as an excitation source and excitation/emission monochromators. Fluorescence emission spectra were measured by exciting the sample at 280 nm and collecting the emission at 330 nm. Experiments were carried out at 25 °C with an entry slit of 0.25 nm and an exit slit of 1.0 nm. Data were recorded at 1 s intervals immediately following the addition of either the complex with the sTFR (yielding a final hTF concentration of 500 nM) or hTF (also 500 nM) alone to a magnetically stirred cuvette containing 1.8 mL at a final concentration of 100 mM MES, pH 5.6, and 4 mM EDTA. As described in the Results, the KCl concentration varied from 150 to 500 mM. It is noteworthy that attempts to measure iron release from the hTF/sTFR complex in the absence of added salt were unsuccessful, presumably due to the tendency of the sTFR to precipitate from solution at pH 5.6 in the absence of salt.

RESULTS

Spectral Analysis. To reduce the complexity and allow comparison of the properties of recombinant hTFs with mutations in the C-lobe triad, all of the constructs contain mutated tyrosine ligands that have been shown previously to eliminate iron binding in the N-lobe (*31*). This strategy simplifies the interpretation of the results, since in the absence of iron binding in the N-lobe any observed iron-binding and iron-release properties can be completely attributed to the C-lobe. Spectral scans of each of the recombinant proteins were taken, since intrinsic spectral parameters (λ_{max} and A_{280}) clearly indicate whether the recombinant proteins are able to bind iron and whether the mutations result in a change in the visible maximum. As shown in Table 2, all of the recombinant proteins had a visible absorbance maximum consistent with specific binding of iron in the C-lobe. The slight upfield shift of λ_{max} in the oTF and LTF triads and downfield shift for the K534R/R632K switch reflect subtle changes in the geometry of the iron-binding site, in particular the relationship of iron to the two tyrosine ligands. We note that, since the triad residues are part of the hydrogen-binding network holding the two subdomains of the C-lobe together, they clearly could have an effect on the visible spectrum.

Table 2: Spectral Scans of Recombinant hTF Proteins

protein	λ_{max} (nm)	A_{280}/A_{max}	note
N-His hTF-NG[a]	464	27.5	diferric
N-His K206E hTF-NG[a]	463	25.6	diferric
N-His Y95F/Y188F hTF-NG[b]	461	42.2	apo-N
N-His Y95F/Y188F/**R632N/D634N** hTF-NG	467	42.2	LTF triad
N-His Y95F/Y188F/**K534R/R632K** hTF-NG	453	44.5	switch
N-His Y95F/Y188F/**K534Q/R632K/D634L** hTF-NG	463	42.8	oTF triad

[a] Reported previously (*13*). [b] Reported previously (*31*).

Table 3: Comparison of Binding Affinities of the Triad Mutants for sTFR at pH 7.4 As Determined by Surface Plasmon Resonance

sample	K_{D1} (nM)	K_{D2}(nM)
hTF-NG	1.84	31.8
Y95F/Y188F hTF-NG	28.5	
Y95F/Y188F "**oTF**" triad hTF-NG	24.2	
Y95F/Y188F "**LTF**" triad hTF-NG	39.4	
Y95F/Y188F "**Switch**" hTF-NG	25.2	

Surface Plasmon Resonance. A surface plasmon resonance (SPR)-based binding assay was used to evaluate the binding affinity of each triad mutant to the soluble portion of the human TFR. Two controls were performed, one with native hTF and one with the Y95F/Y188F hTF NG (monoferric C-lobe). On the basis of the K_D values, obtained for fitting the sensorgram data, the monoferric C-lobe species exhibits a lower affinity for sTFR (Table 3), clearly confirming the preference of sTFR for diferric hTF. Interestingly, a 1:1 binding model, which yields a single K_D value, was sufficient to model the monoferric C-lobe data, whereas a 2:1 bivalent ligand model, which yields two K_D values, is necessary to fit the curves for diferric hTF control (as previously reported) (*29*, *30*). At pH 7.4, the monoferric control has a 15-fold reduced binding affinity compared to K_{D1} of diferric hTF (but bound with an affinity which is similar to K_{D2}). The three triad mutants range from a 0.8- to 1.4-fold change in K_D relative to the monoferric C-lobe control, demonstrating that the composition of the residues at positions 534−632−634 does not substantially alter the strength of the hTF/sTFR interaction in vitro.

Kinetics of Iron Release as a Function of Salt Concentration. Iron-release rates from salt titrations of the hTF proteins containing the human, oTF, LTF, and K534R/R632K triads at pH 5.6 and 25 °C are presented in Figure 1. The mutant containing the three residues found in oTF releases iron marginally faster than does the control N-His Y95F/Y188F hTF-NG and also demonstrates the same increase in the rate constant as a function of increasing KCl. As shown in the inset of Figure 1, when the three residues found in LTF are present, iron release is dramatically slowed and the salt effect is also significantly muted. Additionally, iron release is slowed by the presence of the K534R/R632K switch, although the salt effect is retained.

Kinetic assays were performed on each triad mutant free or bound to sTFR at pH 5.6 in the presence of 300 mM KCl. This pH was chosen because it is the putative

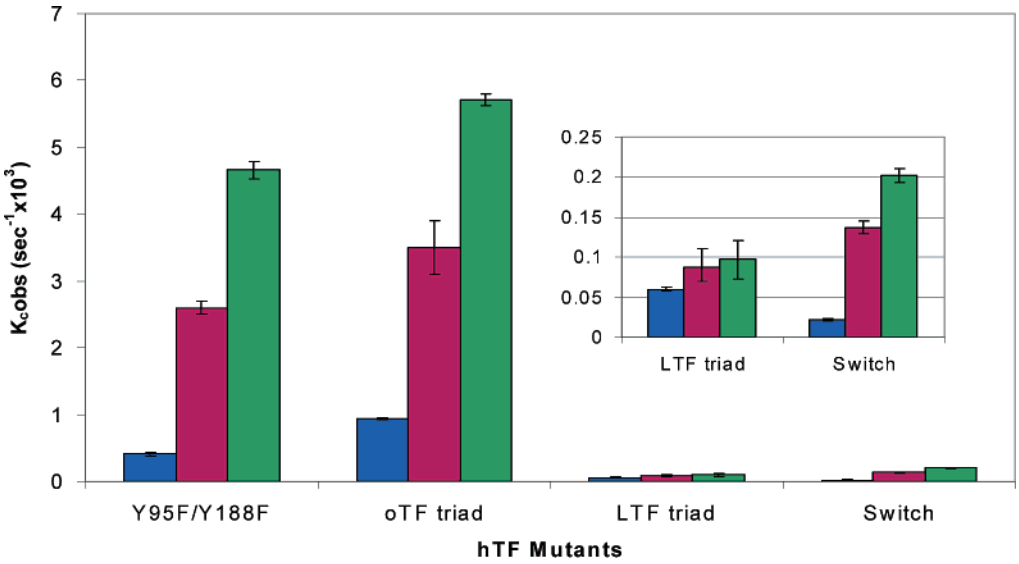

FIGURE 1: Iron-release kinetics for hTF species titrated with KCl. Iron-release rates from the monoferric C-lobe control (N-His Y95F/Y188F hTF-NG) and each of the triad mutants in 100 mM MES, pH 5.6, with 4 mM EDTA as the chelator at 25 °C. Three salt concentrations were used, 0 M (blue), 0.3 M (red), and 0.5 M (green) KCl. The inset expands the *Y*-axis to more clearly show the effect of salt on the iron release rate of LTF and the switch.

Table 4: Kinetics of Iron Release from TFs with and without sTFR[a]

protein[b]		$k_{obs} \pm$ SD[c] ($s^{-1} \times 10^{-3}$)	*n*	fold difference TFR/no TFR
"hTF" triad (K-R-D)		2.6 ± 0.2[d]	4	
	+ TFR	273.0 ± 45[d]	4	105
"oTF" triad (Q-K-L)		3.3 ± 0.1	3	
	+ TFR	91.3 ± 4.7	3	27
authentic oTF C-lobe		1.5 ± 0.002	2	
"LTF" triad (K-N-N)		0.087 ± 0.017	5	
	+ TFR	25.5 ± 0.9	3	195
"switch" triad (R-K-D)		0.136 ± 0.006	4	
	+ TFR	16.5 ± 0.1	3	124
K534A		0.018 ± 0.001	2	
	+ TFR	6.7 ± 0.3	3	364
R632A		too slow		
	+ TFR	2.3 ± 0.1	4	
D634A		too slow		
	+ TFR	too slow		

[a] Iron release from 500 nM hTF at pH 5.6 (100 mM MES, 4 mM EDTA, and 300 mM KCl) in the absence or presence of the soluble TFR at 25 °C. The single point alanine scanning mutants are included for comparisons as is the kinetic rate from the C-lobe of native oTF, all determined under identical conditions. [b] The control is N-HisY95F/Y188F hTF-NG. All constructs are in this background. Note that the triad in hTF is K534/R632/D634. [c] Measurements were carried out as described in Materials and Methods on either a PTI (Photon Technology International QuantaMaster) spectrofluorometer or a Varian Cary 100 dual beam spectrophotometer. [d] Previously reported (*30*).

physiological pH at which receptor-mediated iron release is believed to occur (*3*, *43*). The results (Table 4) show that in all cases binding of the mutants to sTFR dramatically increases the rate of iron release, as observed in previous studies (*26*, *30*). Of the mutants, the oTF "triad" was least affected by the presence of receptor (~27-fold increase in release rate relative to oTF "triad" alone), while the rate of release from wild-type triad, the LTF "triad", and the K534R/R632K switch was accelerated 100-fold or more when TFR was present. Additionally, for comparison, the release rates from the three mutants in which each triad residue is converted to an alanine are included in Table 4. As previously reported (*13*), in each case, this conversion results in a much slower rate of iron release. In fact, under the stated conditions, we were unable to measure any release from the D634A mutant either in the presence or absence of the TFR, and although we were able to obtain a release rate for the other two alanine mutants (K534A and R634A) in the presence of the TFR, the release of iron from the R632A mutant was too slow to measure in its absence.

We have found, as previously reported (*44*), that the release rates measured for selected samples on the PTI and the Cary 100 yield very similar iron release rates regardless of whether they were fluorescence- or absorbance-based (data not shown). From an experimental standpoint, an absorbance-based approach is more convenient over an extended period of time (for example, the LTF and switch triad mutants in the absence of sTFR), because multiple samples can be run simultaneously. Alternatively, the fluorescence-based approach requires a lower concentration of protein, critical for the measurement of the hTF/sTFR complex where solubility is limiting.

Since the recombinant hTF containing the three residues found in LTF released iron so slowly, a salt titration was performed with the complex to determine the release rates in a more experimentally tractable time frame. As shown in Table 5, a marginal salt effect is observed in both the presence and absence of sTFR. In either case (with or without the sTFR), the differences in the observed release rates at the various KCl concentrations are very small compared to the increases observed in the other mutants (Figure 1).

DISCUSSION

A compelling goal of transferrin research is to provide a structural explanation for the well-known differences between family members and between the two lobes of each family member with respect to their thermodynamic and kinetic properties. Over a period of years, detailed studies of iron uptake and iron release from hTF, oTF, and LTF have been undertaken by El Hage Chahine and his colleagues with the aim of elucidating the mechanistic differences between each

Table 5: Salt Titration of LTF-Triad Containing hTF with and without sTFR[a]

protein	[KCl] (mM)	$K_{obs} \pm$ SD ($s^{-1} \times 10^3$)	*n*
R632N/D634N "LTF"	0	0.060 ± 0.002	5
	150	0.113 ± 0.006	3
	300	0.087 ± 0.019	5
	500	0.097 ± 0.027	5
R632N/D634N "LTF"+ TFR	0	could not do	-
	150	19.3 ±0.6	3
	300	25.5 ± 0.9	3
	500	31.6 ±1.6	3

[a] Rate of iron release from the N-His Y95F/Y188F LTF triad in 100 mM MES, pH 5.6, and 4 mM EDTA, at 25 °C as a function of salt concentration.

family member (*22*, *23*, *25*, *45*, *46*). As mentioned in the Introduction, many interesting insights were obtained from this work. The challenge is now to relate the mechanistic details to specific residues within each lobe of each family member. A triad of residues in the C-lobe of hTF has clearly been shown to be important in the mechanism of iron release (*12*, *13*). The key contribution of each member of the triad in iron release is confirmed and extended by the kinetic data for the triad alanine mutants shown in Table 4. Under the stated conditions, the rate of release in the absence of the TFR was too slow to measure for the R632A and D634A mutants and 144-fold slower than the control for the K534A mutant. The current studies were carried out to specifically evaluate the effect of substitution of these three residues with residues found at the equivalent positions in family members, oTF and LTF.

Information on the iron-containing human C-lobe is currently limited to an unrefined 3.3 Å resolution structure (*47*). Fortunately, structures of the closely related pig TF (2.15 Å) and rabbit TF (2.6 Å) are available (*48*), providing a snapshot of the orientation of the three residues in the iron-containing C-lobe. As shown in Table 1, there is a complete conservation of the triad residues in human, pig, and rabbit TF. As depicted in Figure 2, residues Arg632 and Asp634 are in the CI domain, with Lys534 opposite them in the CII domain. For clarity, in the following discussion, human numbering will be used (although the residue numbers for each species are provided in Table 1). The pig structure reveals that there are two potential hydrogen bonds between the aspartic acid and the arginine (both in the CI domain) and a single hydrogen bond between the aspartic acid and the lysine in the CII domain. In the pig structure, the NZ group of the lysine is 4.09 Å from the NE group of the arginine. The lower resolution rabbit structure shows a very similar pattern, although in this case, the lysine NZ group and arginine NE groups are closer (3.3 Å). Additionally, the triad residues reside in a hydrophobic box composed of the three iron-ligands (Tyr426, Tyr517, and His585) as well as the highly conserved Tyr at position 412. As a result, cation-π interactions responsible for the unusual pK_a values noted in the dilysine pair in the N-lobe probably occur here also. In the N-lobe, the ability of the two lysines, Lys206 and Lys296, to share a hydrogen bond is directly attributed to the abnormal pK_a values created by the hydrophobic environment. Likewise, the pK_a values of the residues comprising the triad very likely differ considerably from "normal" values (*19*, *21*).

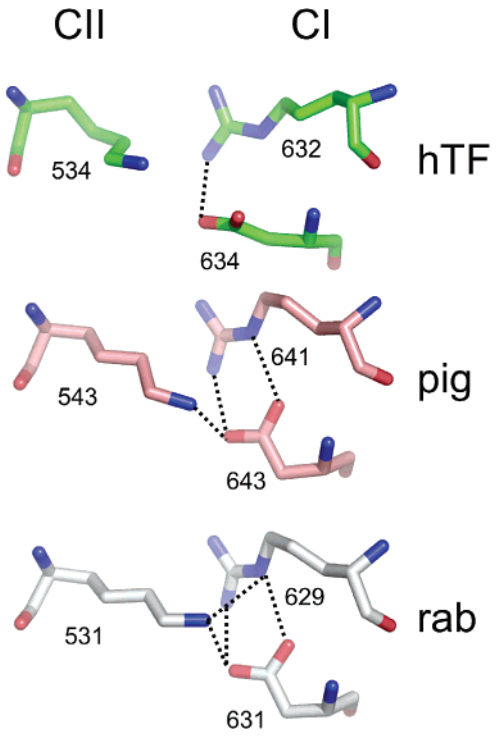

FIGURE 2: Triad residues in TF family members. The diferric structures were obtained from the PDB (1H76 for pig serum TF and 1JNF for rabbit serum TF). Potential H-bonds and residue positions are indicated.

As briefly mentioned in the Introduction, at least two different (but related) pathways have been suggested to describe iron release from the N-lobe (*12*, *21*). Given the considerable sequence similarity between lobes, certain aspects of these pathways also undoubtedly apply to the C-lobe. The decrease in pH within the acidic endosome results in an influx of protons which would be predicted to disrupt the hydrogen bonds between the aspartic acid and the arginine and lysine residues of the hTF triad. The positively charged lysine and arginine residues on opposite sides of the cleft might then repel each other to initiate the opening of the cleft, as suggested for the two lysines in the N-lobe (*12*). Alternatively, Rinaldo and Field (*21*) have proposed a concerted proton transfer such that Arg632 could acquire a proton from either Lys534 (or from a water molecule that is within hydrogen-bonding distance of Lys534 in the pig structure) and subsequently transfer a proton to the nearby tyrosine ligand (Tyr517) disrupting its hold on the iron. According to the model offered by Rinaldo and Field, this transfer is an early step in a concerted release mechanism leading to the break up the hydrogen-bond network within the cleft and allowing entry of a chelator. In both the N- and C-lobe of hTF, this mechanism also appears to involve the histidine ligand which is held in position by interaction with a highly conserved glutamate residue (Glu83 in the N-lobe and Glu410 in the C-lobe, see Table 1). Since Arg632 in the C-lobe has a pK_a that is two units higher than the corresponding lysine (Lys296) in the N-lobe, protonation of the tyrosine ligand would presumably require a lower pH than needed for the N-lobe with its dilysine pair. Similarly, if a water molecule is involved in the process of proton transfer, a more extreme pH would also be required (*21*). Although experimental evidence strongly supports the lower pH requirement for iron removal from the C-lobe (*22*−*24*,

49), distinguishing experimentally between these two mechanisms is difficult. The 4.09 Å distance between the lysine and arginine residues in the C-lobe of the pig structure might appear to favor the second pathway, although reorientation of the Lys−Arg pair in response to anion binding, the change in pH, and/or binding to TFR also may be possible, especially considering the well-known flexibility within the cleft (*48*). In either case, the result is cleft loosening or opening and access of the chelator to the iron within the cleft.

Surprisingly, substitution of the residues found in oTF for the hTF triad only marginally altered the iron-release rate from the C-lobe (Table 4 and Figure 1), despite the lack of conservation of any residues at the equivalent positions (Table 1). The crystal structure of diferric oTF (PDB 1OVT) shows that the OE1 group of the glutamine (equivalent to Lys534) is 2.96 Å from the NZ group of the lysine (equivalent to Arg632), thereby possibly participating in a hydrogen bond linking the CI and CII subdomains (Table 1). For native oTF, the slower rate of iron release from the C-lobe of oTF compared to the N-lobe has been attributed to the difference between the Gln−Lys and Lys−Lys pairs in each lobe, respectively (*50*, *51*). As described above, for the mammalian TFs, these residues in each lobe of oTF exist in a hydrophobic environment comprised of the liganding residues and the highly conserved tyrosine residue (Tyr85 in the N-lobe and Tyr412 in the C-lobe, Table 1) (*52*). In the present study, determination of the rate of iron release for the C-lobe of native oTF under our stated conditions yielded a rate that is approximately half of that measured for the oTF triad in the hTF background (Table 4). Obviously, it is not clear whether placement of the glutamine and lysine residues within the human scaffolding would allow them to interact, since glutamine is shorter than arginine. The absence of the hydrogen bond might explain the faster rate in the oTF "triad" mutant compared to native oTF.

As discussed above, proton transfer from a lysine residue to tyrosine is probably more facile than transfer from the arginine residue found in hTF and might at least partially account for the slightly faster iron release from the oTF "triad" compared to hTF. In the native oTF structure, the leucine residue at the position equivalent to Asp634 has no contact with the lysine or the glutamine residues, thereby invalidating the triad designation. The absence of the negatively charged aspartic acid residue interacting with both the lysine and arginine residues in hTF implies that the pH dependence of iron release from the C-lobe of oTF should be different, although the chemical relaxation experiments do not seem to support this contention (*23*).

To further evaluate the effect of substitution of lysine by glutamine, the iron release rates for the K206Q and K296Q mutants in the N-lobe were examined. The crystal structure (1.8 Å) of the K206Q mutant (*53*) shows that the Gln206 OE1 side chain is 2.9 Å from the NZ of Lys296. Significantly, the rates of iron release from these two mutants are *not* equivalent (450-fold slower for K206Q versus 130-fold slower for K296Q, compared to the wild-type N-lobe), demonstrating the importance of geometry and orientation of the two residues. The rate of release from the N-lobe (in the absence of salt) is 83.0×10^{-3} s^{-1} at pH 5.6 versus 0.183×10^{-3} s^{-1} for the K206Q mutant and 0.633×10^{-3} s^{-1} for the K296Q mutant (*8*). The release rates for these two N-lobe mutants appear to fall into a range with the same order of magnitude as the rates measured for the C-lobe of the hTF and the oTF "triad" (0.383×10^{-3} s^{-1} and 0.933×10^{-3} s^{-1}, respectively, in the absence of salt).

In contrast to the amino acid substitutions made to simulate the residues in oTF, the substitutions made to reproduce the LTF triad (K-N-N) dramatically altered the iron-release kinetics, resulting in a 30-fold slower rate of iron release compared to hTF (Table 4 and Figure 1). As shown in Table 1, the residues in the LTF triad vary at the middle and last positions, with two asparagine residues in place of arginine and aspartic acid, respectively. Significantly, this K-N-N motif is conserved in the C-lobe of the seven LTF sequences published to date (*54*). Examination of the 2.2 Å diferric human LTF structure (PDB 1FCK) reveals that the carbonyl oxygen of the lysine residue shares a hydrogen bond with a threonine residue (equivalent to Thr537 in hTF) (*55*, *56*). The ND2 group of the asparagine residue at the position equivalent to Arg632 in hTF is in potential hydrogen-bonding distance of the OE1 group of the highly conserved Glu410 and the ND1 of the His585 ligand. The asparagine at the position equivalent to Asp634 in hTF does not appear to be in contact with any other residue. Since in the native LTF structure none of the members of the "triad" are in hydrogen-bonding distance with each other, they, like the oTF triad, do not actually comprise a "triad" per se. As mentioned previously, in the N-lobe of hTF, Glu83 (which occupies the equivalent position to Glu410) interacts with the histidine ligand and appears to be involved in the concerted mechanism of iron release (*16*, *21*), a relationship which may be retained in hTF containing the LTF substitutions. However, the apparent absence of interactions between the three residues might be predicted to retard iron release from the LTF "triad" mutant as is observed; there appears to be no possibility of any kind of "triggering" event either by transfer of a proton or repulsion of residues on opposite sides of the cleft.

The K534R/R632K switch also significantly slows iron release from the C-lobe (Figure 2 and Table 4). It is noteworthy that interchanging the identities of two residues that are both positively charged results in altered iron-release properties as well as a 10 nm shift in the absorbance maximum (Table 2). Evidently, the geometry of these residues is just as important as the charge in the mechanism of iron release, reminiscent of work describing the R210K mutation in LTF N-lobe (*57*, *58*) as well as the K206Q and K296Q N-lobe hTF mutants discussed above. It is reasonable that the K534R/R632K switch leads to similar subtle shifts in the neighboring side chains, resulting in the altered functional behavior. Obviously, a structure is needed to determine whether the aspartic acid still interacts with the lysine and arginine residues in their reversed positions, although the slowness in the release rate argues against this.

Complexes with the soluble human TFR and each of the "triad" mutants were prepared, and the rate of iron release was determined. As a first step, it was necessary to show whether introduction of other residues for those comprising the hTF triad had any effect on the ability of the resulting mutants to bind to the TFR. As expected, no significant differences in binding of any of the "triad" mutants to the soluble human TFR were found in our SPR experiments (Table 3). Consistent with previous reports, the monoferric C-lobe control (Y95F/Y188F hTF-NG) exhibited a lower

affinity (15-fold weaker binding) to sTFR than the diferric control (native hTF-NG) (*59*−*61*). Additionally, the mutants with the oTF, LTF, and K534R/R632K conversions bound to sTFR with K_D values similar to the K_D of the control monoferric parent protein. The results are completely consistent with previous studies of the hTF/sTFR interaction in which none of the residues comprising the triad have been implicated in TFR binding (*27*, *28*). Nevertheless, given the dynamic nature of the interaction of hTF with the sTFR, we felt that this needed to be verified experimentally.

In agreement with previous work, the presence of the sTFR significantly accelerates the rate of iron release from the hTF C-lobe at pH 5.6 (*26*, *30*); thus, the rate of iron release from the native human C-lobe of hTF increases at least 100-fold due to the presence of the sTFR. This TFR-induced acceleration is attributed to stabilization of the apo or open/partially open form of hTF which is induced by interaction of His349 with a hydrophobic patch on the TFR (*30*). This work strongly supports earlier suggestions of long-range-induced conformational changes with impact on the iron site. Interestingly, the effect of the TFR on the rate of iron release is considerably less for the oTF triad. The rate of release induced by binding of the oTF "triad" mutant to the sTFR is ∼4-fold lower than the increase observed for the hTF C-lobe in the sTFR complex. This is a significant difference and implies that this "triad" mutant does not achieve the full conformational change required for maximal stimulation of iron release from the C-lobe. It is tempting to attribute some of the difference to the missing aspartic acid residue.

Perhaps most interesting is the LTF mutant (K-N-N) which seems to lack any kind of mechanism to open the cleft and is also missing a robust salt effect (see below), resulting in a 30- fold decrease in the rate of iron release in the absence of the TFR (in comparison to hTF). In the presence of the TFR, the rate of release from the hTF with the LTF triad is increased 230-fold compared to the ∼100-fold enhancement of the rate of release from the C-lobe in the hTF/sTFR complex. Nevertheless, the actual rate is still ∼10-fold slower (0.026 vs 0.273 s^{-1}) (Table 4). Likewise, the rate of iron release from the switch mutant is 120-fold faster when bound to the TFR, although, again, the actual rate is the slowest of any of the triad mutants in complex with the TFR (0.0165 s^{-1}), some 17-fold-slower than the control. Thus, the composition of the triad residues has a very significant effect on the TFR-induced iron release from the C-lobe, reinforcing the idea that the residues in the cleft immediately surrounding the iron site communicate locally but also have a more global response. The extremely slow rate of release observed for the single alanine mutants even in the presence of the TFR (Table 4) confirms the roles of both charge and geometry in the process of iron release. The importance of the aspartic acid residue is highlighted by the fact that no iron release is observed either with or without the TFR in an experimentally feasible time frame.

A further goal of the triad substitutions was the possibility of identifying an anion-binding site in the C-lobe. It has long been known that anionic salts influence chelator-mediated iron removal from hTF (*8*, *10*). Several types of anion interactions have been described, including kinetically significant anions, which are thought to bind at a site or sites near the metal-binding center and change the conformation allowing an incoming chelator to more readily remove the iron (*33*). In the C-lobe, mutation of the lysine at position 569 to glutamine produced a 15-fold decrease in the iron-release rate compared to the control (*62*), indicating that this residue might be a kinetically significant anion binding site (or KISAB site). However, it was also suggested that Lys569 is probably not the only such site in the C-lobe. This conclusion appears to be supported by the fact that in pig TF the lysine at position 569 is replaced by a glutamic acid residue. The lack of conservation in this closely related family member implies that this residue is not essential to iron release (although it clearly has an effect). In the N-lobe, we have shown that the second shell residue network, specifically, the Lys296 and the synergistic anion anchoring Arg124, serve as anion-binding sites (*8*, *10*, *20*). The homologous residues in the C-lobe could similarly play such a role. Kinetic rates from the C-lobes containing the human, oTF, and the K534R/R632K switch "triads" all displayed a significant salt effect in which 6−9.5-fold increases between 0 and 500 mM KCl were observed (Figure 1). In all three constructs, the middle position has a positively charged residue (either a lysine or arginine). Interestingly, the mutant with the LTF substitutions at the triad positions displayed almost no dependence on KCl. To determine whether this mutant had a diminished salt effect or whether the slow iron-release kinetics was masking salt dependence, a salt titration was performed with the mutant/TFR complex (Table 4). Although, in the presence of the TFR, iron release is much more rapid, the effect of increasing the KCl concentration from 150 to 500 mM resulted in less than a 2-fold increase in the rate of iron release. Taken as a whole, the results suggest that the residue in the middle position might well be an anion site, since conversion of this residue to the nonbasic amino acid asparagine (in the LTF mutant) curtails the acceleration of the rate of release by salt. Somewhat surprisingly, we were unable to find any studies examining the effect of salt on iron release from LTF. The absence of a significant salt effect in the LTF highlights yet another fundamental difference to provide an explanation for the slower rate of iron release from native LTF in comparison to hTF. LTF seems ideally suited for its function of sequestering iron and withholding it from invading pathogens.

With the exception of the D634A mutant, none of the substitutions to the hTF triad completely eliminated the effect of the TFR in accelerating iron release, as might be predicted by the fact that all of the mutants retain His349 shown to be critical in this acceleration at acidic pH (*30*). Although neither native oTF nor native LTF bind to the human TFR (*63*), substitution of the three residues which comprise the triad in hTF did not have a significant effect on binding (as was expected). Clearly, in the absence of crystal structures, we do not know the exact relationship of the triad residues when placed in the human scaffolding. Nevertheless, the behaviors of the oTF and LTF mutants are instructive with regard to the importance of the identity of each member of the triad and of the geometry of the site. We note that the K-R-D triad combination in human TF seems particularly well-adapted to acceleration of iron release at pH 5.6 in the presence of the TFR, yielding by far the fastest rate. The aspartic acid residue provides a pH-sensitive element. As mentioned repeatedly, the key to understanding how the dilysine pair in the N-lobe and the triad in the C-lobe exist

is recognizing the hydrophobic environment in which these residues reside. This environment gives rise to unusual pK_a values, which allow anomalous behaviors, increasing or decreasing susceptibility to the protonation events which drive iron release.

REFERENCES

1. Baker, E. N., Baker, H. M., and Kidd, R. D. (2002) Lactoferrin and transferrin: functional variations on a common structural framework, *Biochem. Cell Biol. 80*, 27−34.
2. Aisen, P., Enns, C., and Wessling-Resnick, M. (2001) Chemistry and biology of eukaryotic iron metabolism, *Int. J. Biochem. Cell Biol. 33*, 940−959.
3. Klausner, R. D., Ashwell, G., van Renswoude, J., Harford, J. B., and Bridges, K. R. (1983) Binding of apotransferrin to K562 cells: explanation of the transferrin cycle, *Proc. Natl. Acad. Sci. U.S.A. 80*, 2263−2266.
4. Weinberg, E. D. (1974) Iron and susceptibility to infectious disease, *Science 184*, 952−956.
5. Williams, J. (1968) Comparison of glycopeptides from the ovotransferrin and serum transferrin of the hen, *Biochem. J. 108*, 57−67.
6. Lönnerdal, B., and Iyer, S. (1995) Lactoferrin: molecular structure and biological function, *Annu. Rev. Nutr. 15*, 93−110.
7. Williams, J. (1982) The evolution of transferrin, *Trends Biochem. Sci. 7*, 394−397.
8. He, Q.-Y., and Mason, A. B. (2002) Molecular aspects of release of iron from transferrins, in *Molecular and Cellular Iron Transport* (Templeton, D. M., Ed.) pp 95−123, Marcel Dekker, Inc., New York.
9. Harris, W. R., Cafferty, A. M., Abdollahi, S., and Trankler, K. (1998) Binding of monovalent anions to human serum transferrin, *Biochim. Biophys. Acta 1383*, 197−210.
10. He, Q. Y., Mason, A. B., Nguyen, V., MacGillivray, R. T. A., and Woodworth, R. C. (2000) The chloride effect is related to anion binding in determining the rate of iron release from the human transferrin N-lobe, *Biochem. J. 350*, 909−915.
11. Evans, R. W., Crawley, J. B., Joannou, C. L., and Sharma, N. D. (1999) Iron proteins, in *Iron and Infection: Molecular, Physiological and Clinical Aspects* (Bullen, J. J., and Griffiths, E., Eds.) 2nd ed., pp 27−86, John Wiley and Sons, Chichester, U.K.
12. Dewan, J. C., Mikami, B., Hirose, M., and Sacchettini, J. C. (1993) Structural evidence for a pH-sensitive dilysine trigger in the hen ovotransferrin N-lobe: implications for transferrin iron release, *Biochemistry 32*, 11963−11968.
13. Halbrooks, P. J., He, Q. Y., Briggs, S. K., Everse, S. J., Smith, V. C., MacGillivray, R. T. A., and Mason, A. B. (2003) Investigation of the mechanism of iron release from the C-lobe of human serum transferrin: mutational analysis of the role of a pH sensitive triad, *Biochemistry 42*, 3701−3707.
14. Mason, A. B., Halbrooks, P. J., James, N. G., Connolly, S. A., Larouche, J. R., Smith, V. C., MacGillivray, R. T. A., and Chasteen, N. D. (2005) Mutational analysis of C-lobe ligands of human serum transferrin: insights into the mechanism of iron release, *Biochemistry 44*, 8013−8021.
15. Baker, H. M., Anderson, B. F., Brodie, A. M., Shongwe, M. S., Smith, C. A., and Baker, E. N. (1996) Anion binding by transferrins: importance of second-shell effects revealed by the crystal structure of oxalate-substituted diferric lactoferrin, *Biochemistry 35*, 9007−9013.
16. He, Q.-Y., Mason, A. B., Woodworth, R. C., Tam, B. M., MacGillivray, R. T. A., Grady, J. K., and Chasteen, N. D. (1998) Mutations at nonliganding residues Tyr-85 and Glu-83 in the N-lobe of human serum transferrin−functional second shell effects, *J. Biol. Chem. 273*, 17018−17024.
17. MacGillivray, R. T. A., Moore, S. A., Chen, J., Anderson, B. F., Baker, H., Luo, Y. G., Bewley, M., Smith, C. A., Murphy, M. E., Wang, Y., Mason, A. B., Woodworth, R. C., Brayer, G. D., and Baker, E. N. (1998) Two high-resolution crystal structures of the recombinant N-lobe of human transferrin reveal a structural change implicated in iron release, *Biochemistry 37*, 7919−7928.
18. Jeffrey, P. D., Bewley, M. C., MacGillivray, R. T. A., Mason, A. B., Woodworth, R. C., and Baker, E. N. (1998) Ligand-induced conformational change in transferrins: crystal structure of the open form of the N-terminal half-molecule of human transferrin, *Biochemistry 37*, 13978−13986.
19. Steinlein, L. M., Ligman, C. M., Kessler, S., and Ikeda, R. A. (1998) Iron release is reduced by mutations of lysine 206 and 296 in recombinant N-terminal half-transferrin, *Biochemistry 37*, 13696−13703.
20. He, Q.-Y., Mason, A. B., Tam, B. M., MacGillivray, R. T. A., and Woodworth, R. C. (1999) Dual role of Lys206−Lys296 interaction in human transferrin N-lobe: iron-release trigger and anion-binding site, *Biochemistry 38*, 9704−9711.
21. Rinaldo, D., and Field, M. J. (2003) A computational study of the open and closed forms of the N-lobe human serum transferrin apoprotein, *Biophys. J. 85*, 3485−3501.
22. Abdallah, F. B., and El Hage Chahine, J. M. (1999) Transferrins, the mechanism of iron release by ovotransferrin, *Eur. J. Biochem. 263*, 912−920.
23. Abdallah, F. B., and El Hage Chahine, J. M. (2000) Transferrins: iron release from lactoferrin, *J. Mol. Biol. 303*, 255−266.
24. El Hage Chahine, J. M., and Pakdaman, R. (1995) Transferrin, a mechanism for iron release, *Eur. J. Biochem. 230*, 1102−1110.
25. El Hage Chahine, J.-M., and Fain, D. (1994) The mechanism of iron release from transferrin. Slow-proton-transfer-induced loss of nitrilotriacetatoiron(III) complex in acidic media, *Eur. J. Biochem. 223*, 581−587.
26. Zak, O., and Aisen, P. (2003) Iron release from transferrin, its C-lobe, and their complexes with transferrin receptor: presence of N-lobe accelerates release from C-lobe at endosomal pH, *Biochemistry 42*, 12330−12334.
27. Liu, R. T., Guan, J. Q., Zak, O., Aisen, P., and Chance, M. R. (2003) Structural reorganization of the transferrin C-lobe and transferrin receptor upon complex formation: the C-lobe binds to the receptor helical domain, *Biochemistry 42*, 12447−12454.
28. Cheng, Y., Zak, O., Aisen, P., Harrison, S. C., and Walz, T. (2004) Structure of the human transferrin receptor−transferrin complex, *Cell 116*, 565−576.
29. Giannetti, A. M., Snow, P. M., Zak, O., and Björkman, P. J. (2003) Mechanism for multiple ligand recognition by the human transferrin receptor, *PLoS Biol. 1*, 341−350.
30. Giannetti, A. M., Halbrooks, P. J., Mason, A. B., Vogt, T. M., Enns, C. A., and Björkman, P. J. (2005) The molecular mechanism for receptor-stimulated iron release from the plasma iron transport protein transferrin, *Structure*, in press.
31. Mason, A. B., Halbrooks, P. J., Larouche, J. R., Briggs, S. K., Moffett, M. L., Ramsey, J. E., Connolly, S. A., Smith, V. C., and MacGillivray, R. T. A. (2004) Expression, purification, and characterization of authentic monoferric and apo-human serum transferrins, *Protein Expression Purif. 36*, 318−326.
32. Marques, H. M., Watson, D. L., and Egan, T. J. (1991) Kinetics of iron removal from human serum monoferric transferrins by citrate, *Inorg. Chem. 30*, 3758−3762.
33. Egan, T. J., Ross, D. C., Purves, L. R., and Adams, P. A. (1992) Mechanism of iron release from human serum C-terminal monoferric transferrin to pyrophosphate: kinetic discrimination between alternative mechanisms, *Inorg. Chem. 31*, 1994−1998.
34. Mason, A. B., He, Q. Y., Halbrooks, P. J., Everse, S. J., Gumerov, D. R., Kaltashov, I. A., Smith, V. C., Hewitt, J., and MacGillivray, R. T. A. (2002) Differential effect of a His tag at the N- and C-termini: functional studies with recombinant human serum transferrin, *Biochemistry 41*, 9448−9454.
35. Mason, A. B., Miller, M. K., Funk, W. D., Banfield, D. K., Savage, K. J., Oliver, R. W. A., Green, B. N., MacGillivray, R. T. A., and Woodworth, R. C. (1993) Expression of glycosylated and nonglycosylated human transferrin in mammalian cells. Characterization of the recombinant proteins with comparison to three commercially available transferrins, *Biochemistry 32*, 5472−5479.
36. Williams, S. C., and Woodworth, R. C. (1973) The interaction of iron−conalbumin (anion) complexes with chick embryo red blood cells, *J. Biol. Chem. 248*, 5848−5853.
37. Mason, A. B., He, Q.-Y., Adams, T. E., Gumerov, D. R., Kaltashov, I. A., Nguyen, V., and MacGillivray, R. T. A. (2001) Expression, purification, and characterization of recombinant nonglycosylated human serum transferrin containing a C-terminal hexahistidine tag, *Protein Expression Purif. 23*, 142−150.
38. Lebrón, J. A., Bennett, M. J., Vaughn, D. E., Chirino, A. J., Snow, P. M., Mintier, G. A., Feder, J. N., and Björkman, P. J. (1998) Crystal structure of the hemochromatosis protein HFE and characterization of its interaction with transferrin receptor, *Cell 93*, 111−123.
39. West, A. P., Jr., Giannetti, A. M., Herr, A. B., Bennett, M. J., Nangiana, J. S., Pierce, J. R., Weiner, L. P., Snow, P. M., and Björkman, P. J. (2001) Mutational analysis of the transferrin

receptor reveals overlapping HFE and transferrin binding sites, *J. Mol. Biol. 313*, 385−397.
40. Fagerstam, L. G., Frostell-Karlsson, A., Karlsson, R., Persson, B., and Ronnberg, I. (1992) Biospecific interaction analysis using surface plasmon resonance detection applied to kinetic, binding site and concentration analysis, *J. Chromatogr. 597*, 397−410.
41. Malmqvist, M. (1993) Biospecific interaction analysis using biosensor technology, *Nature 361*, 186−187.
42. Giannetti, A. M., and Björkman, P. J. (2004) HFE and transferrin directly compete for transferrin receptor in solution and at the cell surface, *J. Biol. Chem. 279*, 25866−25875.
43. Sipe, D. M., and Murphy, R. F. (1991) Binding to cellular receptors results in increased iron release from transferrin at mildly acidic pH, *J. Biol. Chem. 266*, 8002−8007.
44. Lehrer, S. S. (1969) Fluorescence and absorption studies of the binding of copper and iron to transferrin, *J. Biol. Chem. 244*, 3613−3617.
45. Pakdaman, R., and El Hage Chahine, J. M. (1996) A mechanism for iron uptake by transferrin, *Eur. J. Biochem. 236*, 922−931.
46. Pakdaman, R., Petitjean, M., and El Hage Chahine, J. M. (1998) transferrins−a mechanism for iron uptake by lactoferrin, *Eur. J. Biochem. 254*, 144−153.
47. Zuccola, H. J. (1993) The crystal structure of monoferric human serum transferrin, Georgia Institute of Technology, Atlanta, GA.
48. Hall, D. R., Hadden, J. M., Leonard, G. A., Bailey, S., Neu, M., Winn, M., and Lindley, P. F. (2002) The crystal and molecular structures of diferric porcine and rabbit serum transferrins at resolutions of 2.15 and 2.60 Å, respectively, *Acta Crystallogr., Sect. D: Biol. Crystallogr. 58*, 70−80.
49. Gumerov, D. R., Mason, A. B., and Kaltashov, I. A. (2003) Interlobe communication in human serum transferrin: metal binding and conformational dynamics investigated by electrospray ionization mass spectrometry, *Biochemistry 42*, 5421−5428.
50. Muralidhara, B. K., and Hirose, M. (2000) Anion-mediated iron release from transferrins−the kinetic and mechanistic model for N-lobe of ovotransferrin, *J. Biol. Chem. 275*, 12463−12469.
51. Mizutani, K., Muralidhara, B. K., Yamashita, H., Tabata, S., Mikami, B., and Hirose, M. (2001) Anion-mediated Fe^{3+} release mechanism in ovotransferrin C-lobe−a structurally identified SO_4^{2-} binding site and its implications for the kinetic pathway, *J. Biol. Chem. 276*, 35940−35946.
52. Kurokawa, H., Mikami, B., and Hirose, M. (1995) Crystal structure of diferric hen ovotransferrin at 2.4 Å resolution, *J. Mol. Biol. 254*, 196−207.
53. Yang, A. H. W., MacGillivray, R. T. A., Chen, J., Luo, Y., Wang, Y., Brayer, G. D., Mason, A. B., Woodworth, R. C., and Murphy, M. E. P. (2000) Crystal structures of two mutants (K206Q, H207E) of the N-lobe of human transferrin with increased affinity for iron, *Protein Sci. 9*, 49−52.
54. Lambert, L. A., Perri, H., and Meehan, T. J. (2005) Evolution of the duplications in the transferrin family of proteins, *Comp. Biochem. Physiol., Part B: Biochem. Mol. Biol. 140*, 11−25.
55. Anderson, B. F., Baker, H. M., Norris, G. E., Rice, D. W., and Baker, E. N. (1989) Structure of human lactoferrin: crystallographic structure analysis and refinement at 2.8 Å resolution, *J. Mol. Biol. 209*, 711−734.
56. Haridas, M., Anderson, B. F., and Baker, E. N. (1995) Structure of human diferric lactoferrin refined at 2.2 Å resolution, *Acta Crystallogr., Sect. D: Biol. Crystallogr. 51*, 629−646.
57. Peterson, N. A., Anderson, B. F., Jameson, G. B., Tweedie, J. W., and Baker, E. N. (2000) Crystal structure and iron-binding properties of the R210K mutant of the N-lobe of human lactoferrin: implications for iron release from transferrins, *Biochemistry 39*, 6625−6633.
58. Peterson, N. A., Arcus, V. L., Anderson, B. F., Tweedie, J. W., Jameson, G. B., and Baker, E. N. (2002) "Dilysine trigger" in transferrins probed by mutagenesis of lactoferrin: crystal structures of the R210G, R210E, and R210L mutants of human lactoferrin, *Biochemistry 41*, 14167−14175.
59. Young, S. P., Bomford, A., and Williams, R. (1984) The effect of the iron saturation of transferrin on its binding and uptake by rabbit reticulocytes, *Biochem. J. 219*, 505−510.
60. Mason, A. B., He, Q.-Y., Tam, B. M., MacGillivray, R. T. A., and Woodworth, R. C. (1998) Mutagenesis of the aspartic acid ligands in human serum transferrin: lobe-lobe interaction and conformation as revealed by antibody, receptor-binding and iron-release studies, *Biochem. J. 330*, 35−40.
61. Evans, R. W., Crawley, J. B., Garratt, R. C., Grossmann, J. G., Neu, M., Aitken, A., Patel, K. J., Meilak, A., Wong, C., Singh, J., Bomford, A., and Hasnain, S. S. (1994) Characterization and structural analysis of a functional human serum transferrin variant and implications for receptor recognition, *Biochemistry 33*, 12512−12520.
62. Zak, O., Tam, B., MacGillivray, R. T. A., and Aisen, P. (1997) A kinetically active site in the C-lobe of human transferrin, *Biochemistry 36*, 11036−11043.
63. Penhallow, R. C., Brown-Mason, A., and Woodworth, R. C. (1986) Comparative studies of the binding and growth-supportive ability of mammalian transferrins in human cells, *J. Cell. Physiol. 128*, 251−260.

BI0518693